The Effect of Column Diameter and Bed Height on Minimum Fluidization Velocity

Akhil Rao and Jennifer S. Curtis
Dept. of Chemical Engineering, University of Florida, Gainesville, FL 32611

Bruno C. Hancock
Pfizer Global Research and Development, Groton, CT 06340

Carl Wassgren
School of Mechanical Engineering, Purdue University, West Lafayette, IN 47907

DOI 10.1002/aic.12161
Published online January 20, 2010 in Wiley Online Library (wileyonlinelibrary.com).

Experiments show that the minimum fluidization velocity of particles increases as the diameter of the fluidization column is reduced, or if the height of the bed is increased. These trends are shown to be due to the influence of the wall. A new, semi-correlated model is proposed, which incorporates Janssen's wall effects in the calculation of the minimum fluidization velocity. The wall friction opposes not only the bed weight but also the drag force acting on the particles during fluidization. The enhanced wall friction leads to an increase in the minimum fluidization velocity. The model predictions compare favorably to existing correlations and experimental data.
 AIChE J, 56: 2304–2311, 2010
Keywords: minimum fluidization velocity, fluidized bed, column diameter, bed height, fluidization

Introduction

As fluidized bed operations have become more popular in industry, there has been a drive to study these beds in greater detail at laboratory scales. Reducing the size of fluidized beds is gaining interest because of the better gas distribution and operability at smaller scales. Micro fluidized beds (MFBs), which were first proposed by Potic et al.,[1] have good mixing and heat transfer capabilities, making them a useful tool for studying various processes like drying, mixing, or segregation,[2–6] as well as reaction kinetics.[7] For example, MFBs are used to investigate fluidization segregation in the pharmaceutical industry where active ingredients are expensive and difficult to obtain during the early stages of development.

Correspondence concerning this article should be addressed to A. Rao at akhil-rao@hotmail.com.

One parameter of particular interest when working with fluidized beds is the minimum fluidization velocity. Many correlations exist for calculating the minimum fluidization velocity.[8–21] The Wen and Yu[22] correlation is the most commonly used correlation for calculating the minimum fluidization velocity and is given as,

$$24.5\left(\frac{Re}{\vartheta}\right)^2+1650\left(\frac{Re}{\vartheta}\right)-\left(\frac{Ar}{\vartheta^3}\right)=0 \tag{1}$$

where

$$Re=\frac{\rho_g(\vartheta d)U_{mf}}{\mu} \quad \text{and} \tag{2}$$

$$Ar=\frac{(\vartheta d)^3(\rho_s-\rho_g)\rho_g g}{\mu^2} \tag{3}$$

where Re is Reynolds number, Ar is the Archimedes number, ϑ is the sphericity, ρ_g is gas density, d is particle diameter, U_{mf} is

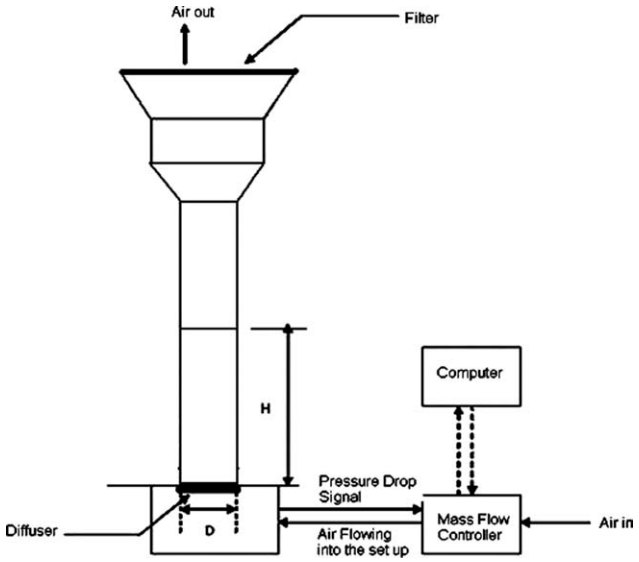

Figure 1. Schematic of the experimental set up.

the minimum fluidization velocity, μ is gas dynamic viscosity, ρ_s is solid density, and g is the gravitational acceleration. None of the correlations include the effect of the bed height or diameter of the column, factors which are likely to be of interest when MFBs are considered.

Two recent investigations, however, have examined the influence of column diameter and bed height. Di Felice and Gibilaro[23] described a method for predicting the pressure drop across a particle bed, taking into account the effect of column diameter. They considered the column to be comprised of two sections: an inner core, where the voidage remains nearly constant, and an outer annular section, where the voidage varies because of the presence of the wall. As there is a difference in the voidage over the cross section of the column, the velocity also varies across the column's cross section. This fact was used to develop a modified Ergun's equation, but this effect is only observed at very small column diameter (D) to particle diameter (d) ratios, i.e. $D/d < 15$.

Delebarre[24] assumed that the fluidizing gas density is a function of the instantanious bed height, which in turn influences the minimum fluidizing velocity. This effect only occurs if the column is very tall. For MFBs, where the columns are short, this effect does not play much of a role.

As will be shown in the following section, experiments in which the bed height and column diameter are varied show that both parameters influence the bed's minimum fluidization velocity. Neither Di Felice and Gibilaro's[23] or Delebarre's[24] models are able to capture the experimental results. The remainder of this article describes the theory and experiments in which a new mechanism is proposed for accounting for bed height and column wall effects.

Experimental Setup

Two fluidization segregation units (Jenike and Johanson, Fluidization Material Sparing—Segregation Tester and Fluidization Segregation Tester), were used in the experiments. The first tester has a column diameter of 1.6 cm and a height of 9.5 cm, and the latter tester has a 2.4 cm diameter column and an 18.5 cm height. Details concerning the operation of the testers are given in Hedden et al.[25] and ASTM D-6941.[26]

A schematic of the experimental set up is shown in Figure 1. The experiments were carried out in both columns. A sintered metal plate with an average pore diameter of 40 μm was used as a gas distributor for both the columns. The air enters the column from the bottom, and its flow rate is controlled by a mass flow controller. The pressure drop across the entire setup was measured with a pressure transducer. The instantaneous pressure drop and velocity data were recorded on a computer.

Experiments were performed with glass and polystyrene particles of different sizes, ranging from 100 to 550 μm. These particles are in the Geldart B class. The particles were carefully sieved, then dried in an oven for 12 h, and finally subject to an antistatic bar (Takk industries) to eliminate accumulated electrostatic charge. The particles were stored in a desiccator so that cohesive forces due to moisture were minimized. To further reduce electrostatic charges that develop during fluidization, a very small amount ($\sim$5 mg) of antistatic powder (Larostat® HTS 905 S, manufactured by BASF Corporation) was mixed with the particles, preceding the experiments. Table 1 summarizes the experimental materials and their properties. The notation used to represent the particle type is: G for glass and P for polystyrene, followed by the average particle size in microns. The values for the dynamic friction coefficients of glass and polystyrene on acrylic (the column wall material) are not readily available and so values of friction coefficients, for glass on glass and polystyrene on polystyrene, obtained from Persson and Tosatti[27] were used in the model calculations.

Before running an experiment, air was passed through the empty column to get a background pressure drop due to the column, diffuser, and the filter sections. Next, the particulate material was weighed and loaded into the column from the top. The height, H, to which the column was filled was

Table 1. Experimental Materials and Properties

Material	Diameter (μm)	Density (kg/m^3)	Sphericity	Coefficient of Friction	Notation
Glass	105–125	2500	0.9	0.4	G116
Glass	210–250	2500	0.9	0.4	G231
Glass	250–300	2500	0.9	0.4	G275
Glass	350–420	2500	0.9	0.4	G385
Glass	420–500	2500	0.9	0.4	G462
Glass	500–600	2500	0.9	0.4	G550
Polystyrene	250–300	1250	0.9	0.5	P275
Polystyrene	300–354	1250	0.9	0.5	P328

recorded. The antistatic powder was mixed with the particles. The air velocity was slowly increased beyond the point of fluidization and then decreased to zero to get the entire pressure drop profile. The point of intersection of the pressure drop line for the fixed bed and the horizontal line for the fully fluidized bed is typically defined as the minimum fluidization velocity. However, just before fluidization, the pressure drop across the bed overshoots the expected value and then decreases to a constant value. Such behavior is expected in columns with a small diameter. This overshoot was not observed during defluidization (Figure 2). Thus, the defluidization pressure drop curve was used to determine the point of fluidization.[7,28] A minimal of three cycles of fluidization and defluidization were carried out to determine an average minimum fluidization velocity. Each experiment was repeated twice and the procedure was repeated for all particle types. The maximum fluctuation observed in the value of U_{mf} was $\sim$7% (for G550 in D = 1.6 cm and H = 4.5 cm; $U_{mf} = 24.5 \pm 0.9$ cm/s). The fairly consistent value of U_{mf} observed over the three cycles and two repetitions show that the trends in U_{mf} are not due to poor gas distribution but rather due to the wall effects. Additionally, gas channeling and maldistribution were not observed through the transparent columns during any of the experiments.

Figures 3–6 present the experimental data for the minimum fluidization velocity (U_{mf}) for the glass and polystyrene particles, obtained from both the columns. In these figures, the Reynolds number at U_{mf} is plotted against the aspect ratio of the bed (H/D). In addition to the experimental data, the plots also include theoretical curves that will be described in the following section. The error bars represent the difference in the reading between two repetitions and not amongst different cycles.

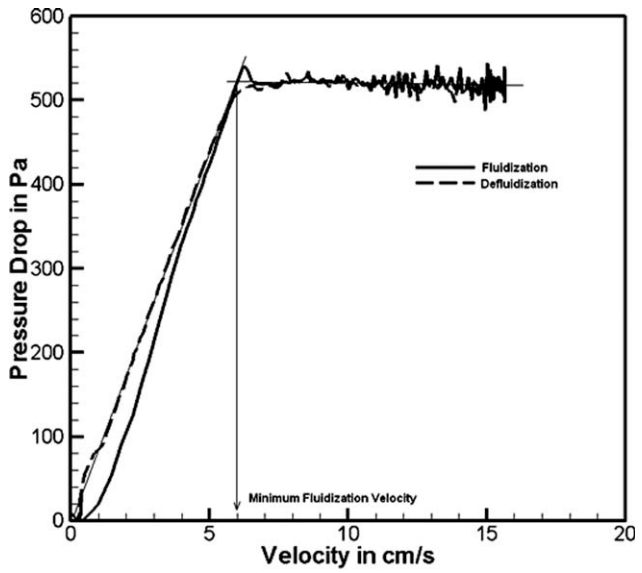

Figure 2. Example of a pressure drop profile (fluidization and defluidization) using G231 particles in the 1.6 cm diameter column.

The minimum fluidization velocity is also shown in the figure.

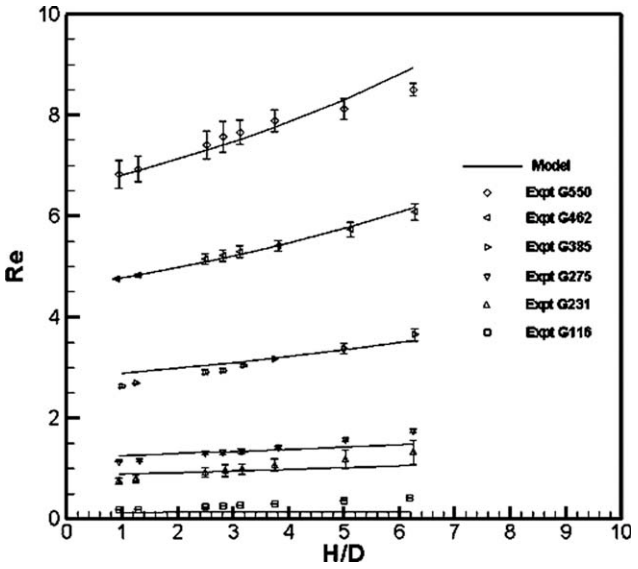

Figure 3. Reynolds number, *Re*, based on the minimum fluidization velocity as a function of aspect ratio, *H/D*, for different glass particles in the 1.6 cm diameter column.

The experimental data (Figures 3–6) show that minimum fluidization velocity monotonically increases as the height of the bed is increased. Further, wall effects on the minimum fluidization velocity are prominent when column diameter, D = 1.6 cm (Figures 3 and 5). While, wall effects on minimum fluidization velocity are much less pronounced for column diameter, D = 2.4 cm (Figures 4 and 6). Although the model proposed by Di Felice and Gibilaro[23] predicts this trend, their model is limited to column to particle diameter ratios of less than 15. In the experiments performed here, this ratio

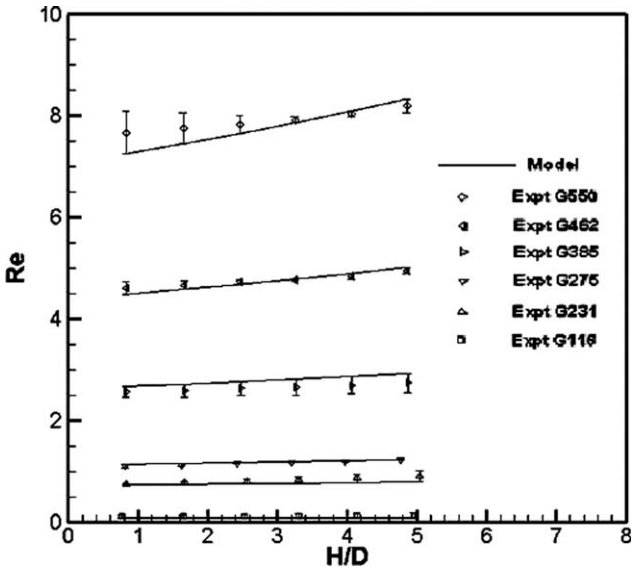

Figure 4. Reynolds number, *Re*, based on the minimum fluidization velocity as a function of aspect ratio, *H/D*, for different glass particles in the 2.4 cm diameter column.

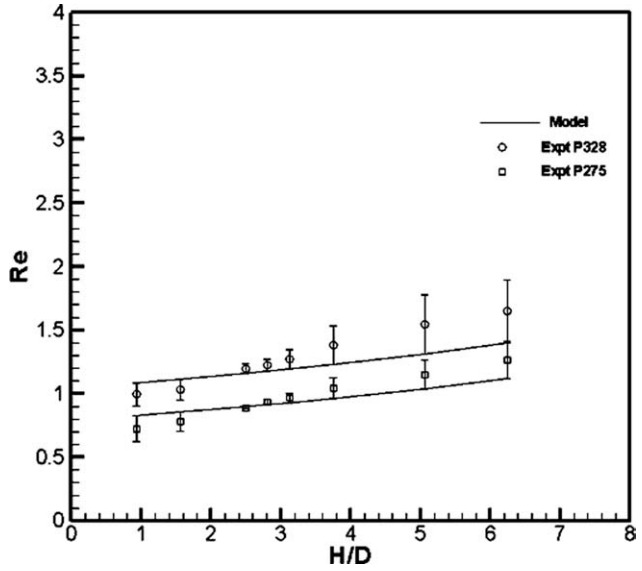

Figure 5. Reynolds number, *Re*, based on the minimum fluidization velocity as a function of aspect ratio, *H/D*, for different polystyrene particles in the 1.6 cm diameter column.

can be as large as 150, well outside the range of validity in Di Felice and Gibilaro's model.

As the height of the bed increases, the minimum fluidization velocity also increases. Delebarre's[24] model accounting for changes in the fluidizing gas density over the bed height predicts at most a minimum fluidization velocity increase of ~0.5%, whereas the observed minimum fluidization velocity increase is greater than 20% in certain cases for the experiments examined here. Thus, this model does not predict the measured data.

Theory

As existing correlations do not include the influence of column diameter or bed height, and because the recent models by Di Felice and Gibilaro[23] and Delebarre[24] do not predict the measured data, a new model is developed in this section to account for the observed trends. As will be presented, a key component of the model is the stress between the column wall and the bed.

The pressure drop, ΔP, for a fixed bed of height, H, is given by the semiempirical correlation of Ergun[16] as:

$$-\frac{\Delta P}{H} = bU + aU^2 \tag{4}$$

where

$$a = 1.75\frac{(1-\in)}{\in^3}\left(\frac{\rho_g}{\vartheta d}\right) \quad \text{and} \tag{5}$$

$$b = 150\frac{(1-\in)^2}{\in^3}\left(\frac{\mu}{\vartheta^2 d^2}\right). \tag{6}$$

The parameter U is the superficial fluid velocity and $\in$ is the bed voidage. The bed void fraction and fluid density are assumed to remain constant throughout the bed.

The pressure drop expression (Eq. 4) can be used to predict the minimum fluidization velocity of a mono-sized material by balancing the pressure force acting on the bed by the effective bed weight.

$$\left[1.75\frac{(1-\in)}{\in^3}\right]Re^2 + \left[150\frac{(1-\in)^2}{\in^3}\right]Re = [(1-\in)Ar] \tag{7}$$

Note that in the previous analysis, the stress between the wall and the bed has not been included.

In the case of a fixed bed with no interstitial fluid, a fraction of the bed weight is supported by the walls of the column. This phenomenon is known as Janssen's wall effect. To determine the wall force acting on the bed, consider a thin horizontal slice of the particle bed of thickness dz (Figure 7). The vertical stress, σ_v, acting on the top face and the weight of the element are balanced by the vertical stress acting on the bottom face and the frictional forces applied by the wall. The resulting differential equation is,

$$\frac{d\sigma_v}{dz} + c_1\sigma_v = c_2 \tag{8}$$

where

$$c_1 = \frac{4tan\varphi k}{D} \quad \text{and} \tag{9}$$

$$c_2 = (1-\in)\rho_s g. \tag{10}$$

The parameter φ is the friction angle between the wall and particles, and D is the column diameter. A horizontal frictional stress, σ_H, arises from the vertical stress, σ_v, producing a wall friction force of $\sigma_H tan\varphi$.[29] It is assumed here

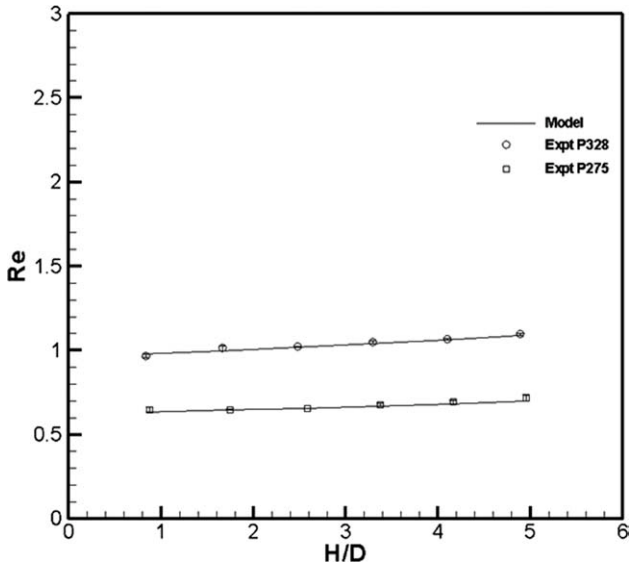

Figure 6. Reynolds number, *Re*, based on the minimum fluidization velocity as a function of aspect ratio, *H/D*, for different polystyrene particles in the 2.4 cm column.

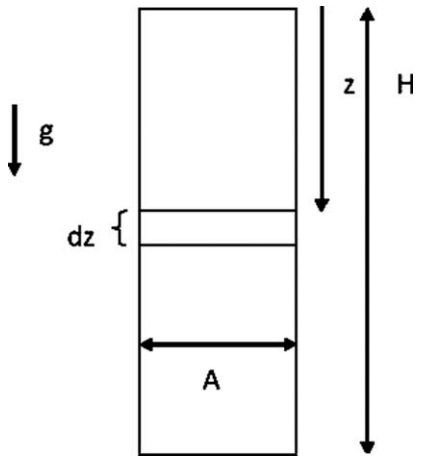

Figure 7. Sketch showing the fluidized bed coordinate system.

that this horizontal stress is directly proportional to the vertical stress with k as the proportionality constant[29]:

$$\sigma_H = k\sigma_v. \tag{11}$$

Solving Eq. 8 subject to the boundary condition that the stress at the top of the bed is zero gives,

$$\sigma_v = \frac{c_2}{c_1}(1 - e^{-c_1 z}). \tag{12}$$

The stress increases nearly linearly near the free surface, but asymptotes to a constant value deeper into the bed. These wall induced stresses will affect the minimum fluidization velocity in narrow columns.

Now consider the situation when fluid is flowing through a fixed bed of solids with the same coordinate system as shown in Figure 7. At equilibrium, the force due to stress on the top face of the element, F_T, and the weight of the element, F_W, will be balanced by the force due to the stress on the bottom face, F_B, the wall friction, F_F (Janssen's effect), the drag force on the solids, F_D, and the buoyancy force, F_{Bu}. Thus, a force balance on the solids yields:

$$F_B + F_F + F_D + F_{Bu} = F_T + F_W \tag{13}$$

which, when expanded is

$$\frac{\pi}{4}D^2(\sigma_v + d\sigma_v) + (tan\varphi\sigma_H)\pi D dz + \frac{\pi}{4}D^2 dp = \frac{\pi}{4}D^2\sigma_v + ((1-\in)(\rho_s - \rho_g)g)\frac{\pi}{4}D^2 dz. \tag{14}$$

In the above expression, F_w and F_{Bu} have been combined to give the last term on the right hand side of Eq. 14. Simplifying and rearranging the previous equation gives,

$$\frac{d\sigma_v}{dz} + \frac{4tan\varphi\sigma_H}{D} = \left[(1-\in)(\rho_s - \rho_g)g - \frac{dp}{dz}\right]. \tag{15}$$

If $\sigma_H = k\sigma_v$ is assumed, as in Eq. 11,

$$\frac{d\sigma_v}{dz} + \frac{4tan\varphi k\sigma_v}{D} = \left[(1-\in)(\rho_s - \rho_g)g - \frac{dp}{dz}\right] \tag{16}$$

which may be written as

$$\frac{d\sigma_v}{dz} + c_1\sigma_v = c_2 \tag{17}$$

where

$$c_1 = \frac{4tan\varphi k}{D} \quad \text{and} \tag{18}$$

$$c_2 = \left[(1-\in)(\rho_s - \rho_g)g - \frac{dp}{dz}\right]. \tag{19}$$

In Eq. 19 there are two additional terms as compared with Eq. 10: the drag term, represented by dp/dz, and the buoyancy term.

The solution to Eq. 17 is equivalent to that of Eq. 8

$$\sigma_v = \frac{c_2}{c_1}(1 - e^{-c_1 z}) \tag{20}$$

but with different c_1 and c_2.

Figure 8 presents Eq. 20 in graphical form. When the velocity is zero (i.e., there is no gas flowing through the column), then Eq. 20 simplifies to Janssen's equation. As the velocity increases, the vertical contact stresses in the bed are smaller because the drag on the particles supports a fraction of the bed's weight. At and above the point of fluidization, the stresses in the column are zero (as contact does not exist

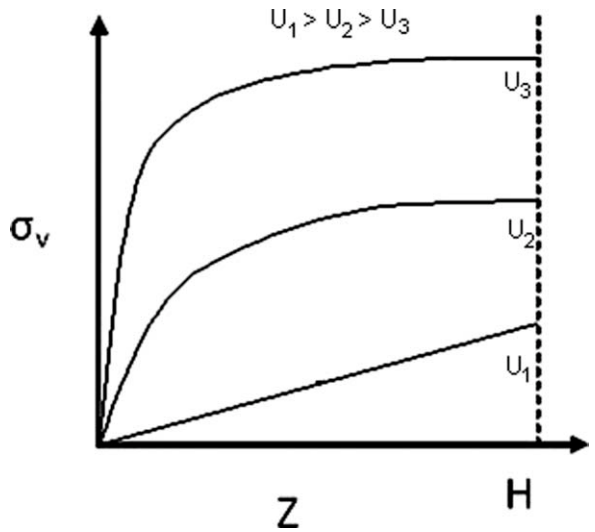

Figure 8. A schematic showing how the vertical stress in the bed varies with bed depth at different fluid velocity U_1, U_2, and U_3.

amongst the particles), and thus $d\sigma_v/dz$ is also zero. This situation is only possible if $c_2 = 0$,

$$c_2 = \left[(1-\in)(\rho_s - \rho_g)g - \frac{dp}{dz}\right] = 0 \tag{21}$$

In Eq. 21, if Ergun's pressure drop expression is substituted (Eq. 4), the resultant expression will be the same as Eq. 7, and the wall effects will not be included in the analysis.

It is now assumed that the horizontal stress is not only a function of the downward vertical stress but also a function the upward drag forces caused by the gas flowing through the column. As Ergun's pressure drop equation is used to calculate the pressure drop, it is assumed that the structure of these new terms on which the horizontal stress depends is similar in form to those given by Ergun's equation, but the velocity terms are being scaled differently. These scales are chosen as they give a favorable fit to the experimental data.

$$\sigma_H = k\sigma_v - k_1 H\left(\frac{\mu}{D\vartheta d}\right)U - k_2 H\left(\frac{\rho_g}{D}\right)U^2 \tag{22}$$

where k_1 and k_2 are constants.

Substituting Eq. 22 back into Eq. 15, yields:

$$\frac{d\sigma_v}{dz} + \frac{4tan\varphi k\sigma_v}{D} = \left[\frac{4tan\varphi k_2(\rho_g)(\frac{H}{D})}{D}\right]U^2 + \left[\frac{4tan\varphi k_1\left(\frac{\mu}{\vartheta d}\right)(\frac{H}{D})}{D}\right]U + \left[(1-\in)(\rho_s-\rho_g)g\right] - \frac{dp}{dz}. \tag{23}$$

Comparing Eq. 23 to Eq. 16, there are two additional terms, proportional to U^2 and U, appearing on the right hand side of Eq. 23. These terms have come about due to the horizontal stress from the wall and the flow of the fluid through the bed.

Substituting Ergun's equation for pressure drop (Eq. 4) into Eq. 23:

$$\frac{d\sigma_v}{dz} + \frac{4tan\varphi k\sigma_v}{D} = \left[\frac{4tan\varphi k_2(\rho_g)(\frac{H}{D})}{D} - a\right]U^2 + \left[\frac{4tan\varphi k_2\left(\frac{\mu}{\vartheta d}\right)(\frac{H}{D})}{D} - b\right]U + \left[(1-\in)(\rho_s-\rho_g)g\right]. \tag{24}$$

This equation is again of the form:

$$\frac{d\sigma_v}{dz} + c_1\sigma_v = c_2 \tag{25}$$

where:

$$c_1 = \frac{4tan\varphi k}{D} \quad \text{and} \tag{26}$$

$$-c_2 = \left[a - \frac{4tan\varphi k_2(\rho_g)(\frac{H}{D})}{D}\right]U^2 + \left[b - \frac{4tan\varphi k_2\left(\frac{\mu}{\vartheta d}\right)(\frac{H}{D})}{D}\right]U - \left[(1-\in)(\rho_s-\rho_g)g\right]. \tag{27}$$

Setting $c_2 = 0$, the condition which is necessary for fluidization, and integrating over the length of the column:

$$\left[a - \frac{4tan\varphi k'_2(\rho_g)(\frac{H}{D})}{D}\right]U^2 + \left[b - \frac{4tan\varphi k'_1\left(\frac{\mu}{\vartheta d}\right)(\frac{H}{D})}{D}\right]U - \left[(1-\in)(\rho_s-\rho_g)g\right] = 0 \tag{28}$$

where k'_1 and k'_2 are lumped parameters which also include integration coefficients. Substituting for a and b, which are Ergun's constants, yields;

$$\left[1.75\frac{(1-\in)}{\in^3} - 4tan\varphi k'_2\left(\frac{\vartheta d}{D}\right)\left(\frac{H}{D}\right)\right]\frac{\rho_g U^2}{\vartheta d} + \left[150\frac{(1-\in)^2}{\in^3} - 4tan\varphi k'_1\left(\frac{\vartheta d}{D}\right)\left(\frac{H}{D}\right)\right]\frac{\mu U}{(\vartheta d)^2} = \left[(1-\in)(\rho_s-\rho_g)g\right] \tag{29}$$

Multiplying throughout by the factor $\frac{\rho_g(\vartheta d)^3}{\mu^2}$ to make the equation dimensionless gives:

$$\left[1.75\frac{(1-\in)}{\in^3} - 4tan\varphi k'_2\left(\frac{\vartheta d}{D}\right)\left(\frac{H}{D}\right)\right]Re^2 + \left[150\frac{(1-\in)^2}{\in^3} - 4tan\varphi k'_1\left(\frac{\vartheta d}{D}\right)\left(\frac{H}{D}\right)\right]Re = \left[(1-\in)Ar\right] \tag{30}$$

Equation 30 is a quadratic equation that can be easily solved for Re, with k'_1 and k'_2 remaining constant. Rewriting Eq. 30 results in

$$a''\left(\in, \varphi, \left(\frac{\vartheta d}{D}\right), \left(\frac{H}{D}\right)\right)Re^2 + b''\left(\in, \varphi, \left(\frac{\vartheta d}{D}\right), \left(\frac{H}{D}\right)\right)Re - (1-\in)Ar = 0 \tag{31}$$

where a'' and b'' are functions not only of $\in$ and φ but also of $(\vartheta d/D)$ and (H/D). Hence, both the ratio of particle size to column diameter $(\vartheta d/D)$ and the bed aspect ratio (H/D) play a role in determining U_{mf}.

Results and Discussion

The values of the universal constants k'_1 and k'_2 which give the minimum error for the experimental data set presented in this study were found out to be 610 and 30.1, respectively. In Figures 3–6 and Figures 9 and 10, the values of the universal constants k'_1 and k'_2 are kept at these values for all of the particle types, bed heights, and column diameters.

Figures 3–6 show that including the wall effects in the prediction of U_{mf} is successful in describing the effects of height vs. column diameter (H/D) and the effect of particle size to column diameter (d/D). The model only slightly under-predicts the increase in U_{mf} for very small sized particles ($d < 120$ μm) in the column with $D = 1.6$ cm, which is likely due electrostatic cohesive and adhesive forces.

For a fixed column diameter, as the H/D ratio increases, U_{mf} increases (Figures 3–6). Hence, as the column becomes taller in comparison to its diameter, the wall effects are more prominent, making it more difficult to fluidize the

particles. Also, for a constant particle size, as d/D ratio increases (due to changes in column diameter), U_{mf} increases (compare Figures 3 and 4 or Figures 5 and 6). As the column diameter decreases in comparison to the particle diameter, the ratio of wall contact surface area to the bulk volume increases, leading to a more significant wall effect. This wall effect reduces as the column increases in diameter relative to the particles, and eventually becomes negligible as d/D becomes very small. The effect of H/D and d/D on U_{mf} are very similar; in fact, the increase in U_{mf} can be characterized by the product of H/D and d/D (Eq. 30). Additionally, as particle size increases and approaches the same order of magnitude as the column diameter ($d/D \sim O(1)$), then fluidization becomes difficult. Above a certain d/D ratio, the particle mixture is impossible to fluidize. This situation is predicted by the model, as the quadratic equation yields complex roots. Similarly, Eq. 30 breaks down for large H/D ratio predicting that at large H/D the gas may not fluidize the bed. For example, the model predicts that if glass particles of size 250 μm are fluidized in a 760 μm diameter column ($D/d \sim 3$) with $H/D = 1$, then the particles will not fluidize. Similarly, the model also predicts that if these particles are loaded into a 100 cm diameter column to a bed height of about 13 m ($H/D \sim 13$), the gas may not fluidize the bed.

Figure 9 compares the experimental data from Liu et al.[7] to the values predicted by the model. The data are plotted in the same dimensional form as given in the orignal work of Liu et al.[7] The model does not predict the increase in U_{mf} for the smaller particles ($d = 96.4$ μm), but it does give good predictions for the larger particle sizes. In this case also, the values of k'_1 and k'_2 are maintained at 610 and 30.1, respectively. For the largest particles ($d = 460$ μm), the prediction for the smallest diameter column is not that good, but this may be due to experimental error, which is not reported in Liu et al.[7] Also, the values of voidage were not clearly stated; only values of bulk density were given. In the model, the values of bulk density were kept constant with respect to the column diameter, but it has been observed that this value changes depending on the column diameter,[28] particularly for small column diameters.

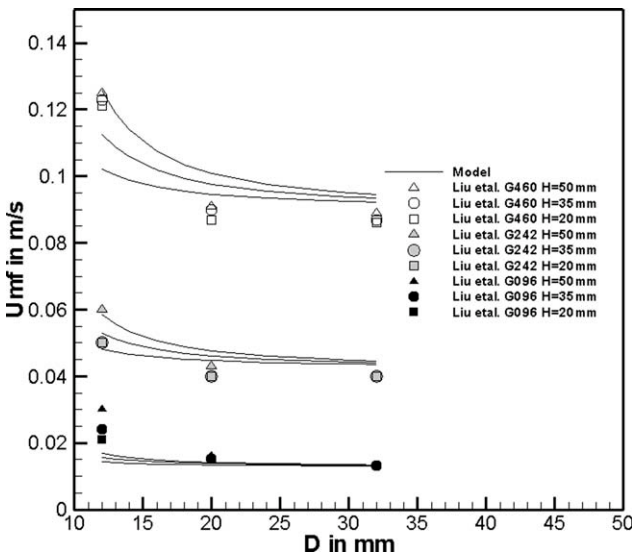

Figure 9. The minimum fluidization velocity as a function of the column diameter using the experimental data from Liu et al.[7]

The curves are from Eq. 30.

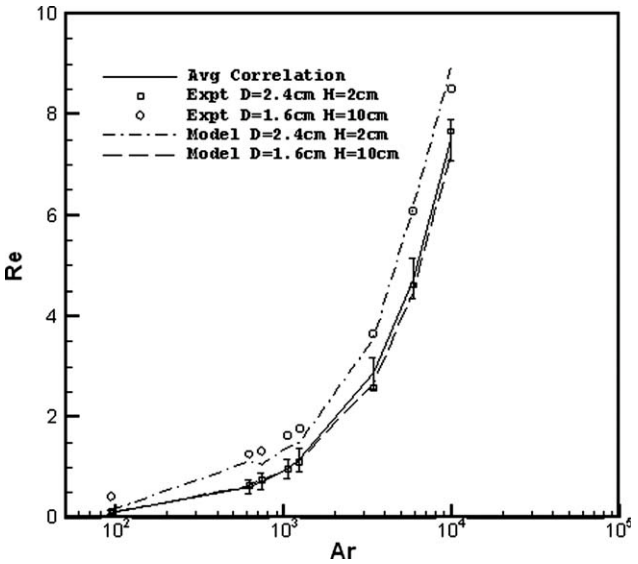

Figure 10. Comparison of the curves from Eq. 30 to the experimental data and existing correlations.

Figure 10 compares the model results to the average predictions of the Reynolds number at U_{mf} based on a large number of existing correlations.[8–22] The scatter bars on the correlation line represent the deviation in minimum fluidization velocity predictions using the different correlations. The experimental data obtained when the wall effects are minimum (at $H = 2$ cm and $D = 2.4$ cm) are consistent with the model prediction and with the averaged correlation curve. On the other hand, only the new model is able to predict experimental data obtained when the wall effects are significant (at $H = 10$ cm, $D = 1.6$ cm), as the existing correlations for U_{mf} do not take wall effects into account.

Conclusions

Experiments show that wall effects influence the minimum fluidization velocity. Existing correlations fail to incorporate these wall effects and, hence, there is a need for a new model that can take these effects into consideration. The model presented in this study attempts to include the wall influence by introducing Janssen's wall effect in the force balance during fluidization. It is assumed that the horizontal stresses acting at the wall are not only a function of the local vertical stress but also are a quadratic function of velocity. These new terms have the same structure as that of the drag term, i.e., the pressure drop, as given by the widely accepted Ergun equation. This assumption leads to a modified Ergun's equation incorporating two universal constants. The new model fits experimental data reasonably well for the minimum fluidization velocity over a range of particles sizes, bed heights, and column diameters. Some deficiencies in the model predictions are noted for smaller particles (around 100 μm and smaller), but these deficiencies may be due to

the significance of cohesive and adhesive forces at this scale. This new model should greatly facilitate scaling results from MFBs to more traditional fluid bed sizes.

Acknowledgments

Jim Prescott and colleagues at Jenike and Johanson are thanked for their support of this research and for providing the segregation testing equipment.

Notation

ϵ = voidage
ϑ = sphericity
μ = viscosity
ρ_g = density of gas
ρ_s = density of solid
σ_H = stress in horizontal direction
σ_v = stress in vertical direction
φ = friction angle
Δp = pressure drop
a, b = Ergun constants
A = cross-sectional area
a', b', c' = various constants of the quadratic
Ar = Archimedes number
D = column diameter
d = particle diameter
F = force
g = Gravity
H = height of fixed bed
$k, k_1, k_2, k_1', k_2', c_1, c_2$ = various constants
Re = Reynolds number
U = fluid velocity
U_{mf} = Minimum Fluidization velocity
z = instantaneous height measured from the top of the bed

Literature Cited

1. Potic B, Kerstn S, Ye M, Van der Hoef M, van Swaaij W. Fluidization of hot compressed water in micro reactors. *Chem Eng Sci*. 2005;60:5982–5990.
2. Chiba S, Nienow A, Chiba T, Kobayashi H. Fluidized binary mixtures in which denser component may be flotsam. *Powder Technol*. 1980;26:1–10.
3. Garcia F, Romero A, Villar J, Bello A. A study of segregation in a gas solid fluidized bed: particles of different density. *Powder Technol*. 1989;58:169–174.
4. Huilin L, Yurong D, Gidaspow D, Lidan Y, Yukun Q. Size segregation of binary mixture of solid in bubbling fluidized bed. *Powder Technol*. 2003;134:86–97.
5. Joseph G, Leboreiro J, Hrenya C, Stevens A. Experimental segregation profiles in bubbling gas fluidized bed. *AIChE J*. 2007;53:2804–2813.
6. Geldart D, Baeyens J, Pope D, Van De Wijer P. Segregation in beds of large particles at high velocity. *Powder Technol*. 1981;30:195–205.
7. Liu X, Xu G, Gao S. Micro fluidized beds: wall effects and operability. *Chem Eng J*. 2008;137:302–307.
8. Babu S, Shah B, Talwalker A. Fluidization correlation for coal gasification materials—minimum fluidization velocity and fluidized bed expansion. *AIChE Symp Ser*. 1978;74:176–186.
9. Baerg A, Klassen J, Gishler P. Heat transfer in a fluidized solid bed. *Can J Res Sect F*. 1950;28:287.
10. Broadhurst T, Becker H. Onset of fluidization and slugging in beds of uniform particles. *AIChE J*. 1975;21:238–247.
11. Davies L, Richardson J. Gas interchange between bubbles and the continuous phase in a fluidized bed. *Trans Inst Chem Eng*. 1966;44:293–305.
12. Goroshko V, Rozenbaum R, Todes O. *Hydrodynamics and Heat Transfer in fluidized beds*. Cambridge: M.I.T. Press, 1966.
13. Grewal N, Saxena S. Comparision of commonly used correlations for minimum fluidization velocityof small solid particles. *Powder Technol*. 1980;26:229–234.
14. Johnson E. Institute of gas engineers report, Publication No. 318. London, 1949.
15. Kumar P, Sen Gupta P. Prediction of minimum fluidization velocity for multicomponent mixtures (short communication). *Indian J Technol*. 1974;12:225.
16. Kunii D, Levenspiel O. *Fluidization Engineering*, 2nd ed. Newton: Butterworth-Heinemann, 1991.
17. Leva M. *Fluidization*. New York: McGraw-Hill, 1959.
18. Miller C, Longwinuk A. Fluidization studies of solid particles. *Ind Eng Chem*. 1951;43:1220–1226.
19. Pillai B, Raja Rao M. Pressure drop and minimum fluidization velocities of air-fluidized bed. *Indian J Technol*. 1971;9:77.
20. Saxena S, Vogel G. The measurement of incipient fluidization velocities in a bed of coarse dolomite at temperature and pressure. *Trans Inst Chem Eng*. 1977;55:184–189.
21. van Heerdeen C, Nobel A, Krevelen v. Studies on fluidization ll—heat transfer. *Chem Eng Sci*. 1951;1:51–66.
22. Wen C, Yu Y. Mechanics of fluidization. *Chem Eng Prog Symp*. 1966;62:100–111.
23. Di Felice R, Gibilaro L. Wall effects for the pressure drop in fixed beds. *Chem Eng Sci*. 2004;59:3037–3040.
24. Delebarre A. Does the minimum fluidization exist? *J Fluid Eng*. 2002;124:595–600.
25. Hedden D, Brone D, Clement S, McCall M, Olsofsy A, Patel P, Prescott J, Hancock B. Development of an improved fluidization segregation tester for use with pharmaceutical powders. *Pharm Technol*. 2006;30:54–64.
26. ASTM International. Standard practice for measuring fluidization segregation tendencies of powders, ASTM International, D6941–03, 2003.
27. Persson B, Tosatti E. *Physics of Sliding Friction (NATO Science Series E)*. New York: Springer Publishing Company, 1966.
28. Loezos P, Costamagna P, Sundaresan S. The role of contact stresses and wall friction on fluidization. *Chem Eng Sci*. 2002;57:5123–5141.
29. Janssen HA. Versuche uber getreidedruck in silozellen. *Z Ver Deutsch Ing*. 1895;39:1045–1049.

Manuscript received Aug. 14, 2009, and revision received Dec. 1, 2009.